JOURNAL OF MATERIALS SCIENCE **39** (2004) 5067–5070

Glass-forming ability determined from inter-atomic potentials for some miscible/immiscible binary metal systems

B. X. LIU*, H. R. GONG, H. B. GUO, L. T. KONG
Advanced Materials Laboratory, Department of Materials Science and Engineering, Tsinghua University, Beijing 100084, People's Republic of China
E-mail: dmslbx@tsinghua.edu.cn

The present study attempts to clarify one of the important issues in the field of metallic glasses (or amorphous alloys), i.e., to predict the glass-forming ability/range (GFA/GFR) of the binary metal systems. Firstly, a brief summary of the experimental observations indicates that in the miscible/immiscible systems, amorphous alloys can be formed in a broad composition range extending from central portion to nearby the edges of the two terminal solid solutions. Consequently, to predict RFA/GFR of a system becomes an issue of determining the critical solid solubility of the system, beyond which a solid solution would collapse into an energetically favored amorphous state. Secondly, the *n*-body potentials are derived by routine methods for the miscible Ni-Ta, Ni-Mo, and Ni-Ti systems, whereas for the immiscible Ag-Co and Cu-W systems having no any equilibrium alloy, the cross potentials are fitted to some physical properties acquired by first principles calculation for a few possible nonequilibrium alloys. Thirdly, applying the proven realistic potentials, molecular dynamics simulations with solid solution models reveal that the physical origin of crystal-to-amorphous transition is the lattice collapsing while solute atoms exceeding the critical solid solubility and that the GFRs of the systems are within the composition ranges bounded by the two determined critical solid solubilities. It turns out that the predictions are in good agreement with the experimental observations.

1. Introduction

In 1960, Duwez *et al.* obtained the first amorphous alloy (or metallic glass) by liquid melt quenching (LMQ) technique in the Au-Si system [1]. In LMQ, the metallic glass is formed through a liquid-to-solid phase transition. Since early 1980s, two unique schemes have been introduced to produce metallic glasses, i.e., ion beam mixing (IBM) and solid-state reaction (SSR) of multiple metal layers [2, 3]. In IBM and SSR, the metallic glasses are formed through a solid-solid phase transition, differing from that involved in LMQ. IBM and SSR have significantly extended the capability in producing metallic glasses and obtained a great number of new amorphous alloys in the binary metal systems [4, 5]. For instance, IBM and SSR are able to produce metallic glasses in the equilibrium immiscible systems characterized by a large positive heat of formation (ΔH_f) defined in Miedema's thermodynamic model [4]. In contrast, in such immiscible systems, LMQ is even not able to form any alloy. A question was then raised that the previously defined glass-forming ability (GFA) mainly based on the experimental data from LMQ should somehow be redefined and developed.

Based on the extensive data accumulated during the past decades concerning the amorphous alloy formation, Liu *et al.* have proposed to define the glass-forming range (GFR) as a quantitative measure for the GFA of a binary metal system. An experimentally determined GFR of a system certainly depends on the specific producing technique applied and is therefore considered as a nominal GFA of the system. From a physical point of view, a binary metal system should have its intrinsic GFA/GFR, which is determined by some internal characteristics of the system. Naturally, the nominal GFR is frequently smaller than the intrinsic GFR and the greater the GFR observed by a specific technique, the closer the nominal GFR to the intrinsic GFR. It has been shown that IBM is a powerful scheme to produce metallic glasses in the binary metal systems and the GFR determined by IBM could be within a broad composition range, extending from the central portion to nearby the edges of the two terminal solid solutions. Based on IBM results, Liu *et al.* have proposed to predict the GFR of a system to be within the maximum possible amorphization range (MPAR) of the system, which equals the whole composition range minus the two maximum

*Author to whom all correspondence should be addressed.

terminal solid solubilities. In other words, the composition range bounded by the two maximum solid solubilities is the GFR/GFA of the system [5]. It follows that to predict the GFR of a system is thus transferred to an objective of determining the maximum solid solubilities, namely the critical compositions of crystal-to-amorphous transitions, which divide the composition range of the system into three regions energetically favoring the solid solutions and the disordered states, respectively. From a structural point of view, the energetic states of both solid solutions and disordered states are determined by their respective atomic configurations, which are governed by the intrinsic atomic potential of the system. Consequently, if a realistic potential of a system is first constructed, the critical solid solubilities of the system can be determined by performing molecular dynamics (MD) simulation using solid solution models to compare the energetic levels of the solid solution versus the disordered state as a function of the alloy composition. The present study is dedicated to determine the intrinsic GFR of some miscible/immiscible binary metal systems from the respective inter-atomic potentials through molecular dynamics simulations.

2. Construction of the *n*-body potentials

To perform MD simulation in a binary metal system, a realistic potential for the system is necessary and should first be constructed. Previously, the pair potential has been the most popular approach applied in computer simulation, though it has some drawbacks. Since early 1980s, the problem has been solved with the emergence of the so-called n-body models. In 1983, Daw and Baskes proposed an approach named embedded-atom method (EAM), in which the interaction between two atoms was correlated not only to the interatomic distance but also to the local environment around the atom [6]. The basic idea of the EAM can be interpreted under the framework of density-functional theory, from which the energy required to place an impurity atom into a lattice is determined solely by the electron density at that particular site, without considering the origin of the electron density [6]. In addition to the EAM potential, another two methods have been proposed for the transition metals, i.e., the Finnis-Sinclair (FS) potential [7] and the tight-binding (TB) potential [8]. The FS and TB models are both based on the tight-binding theory of cohesion by assuming that the band energy is a sum of the occupied one-electron energies in a band, which is proportional to the square root of the second moment of its density of states [7, 8].

We first discuss the construction of the n-body potentials for some miscible systems with negative heat of formation (ΔH_f). In the present study, the Ni-Ta, Ni-Mo, and Ni-Ti systems are selected and their respective ΔH_f are -44, -11, and -52 kJ/mol [9]. Accordingly, we adopt EAM, FS, and TB potential forms for the Ni-Ta, Ni-Mo, and Ni-Ti systems, respectively, to derive their n-body potentials. It should be noted that the potential parameters of these miscible systems are fitted to the available experimental data of the systems. Take the Ni-Mo system as an example, Table I displays the fitted parameters for the Ni-Ni, Mo-Mo, and Ni-Mo potentials based on the Finnis-Sinclair formalism. The construction as well as the fitting process of these potentials has been published elsewhere [10–12].

TABLE I Parameters for the Ni-Ni, Mo-Mo, and Ni-Mo potentials

	Ni-Ni	Mo-Mo	Ni-Mo
A (eV)	1.042095	1.883457	1.144552
d (Å)	4.0	4.114825	5.25
c (Å)	3.72	3.25	4.05
C_0	2.1853329	43.4475218	49.418638
C_1	−0.6346408	−31.9332978	−60.373527
C_2	−0.4184836	6.0804249	27.366179
C_3	0.1364786	0.0	−5.388922
C_4	0.0	0.0	0.387794

We now discuss the potential construction for two representative equilibrium immiscible systems, i.e., the Co-Ag and Cu-W systems. For the Co-Ag system with a ΔH_f of +28 kJ/mol [9], we adopt the TB formalism proposed by Tomanek *et al.* [8]. For the Cu-W system with a ΔH_f of +33 kJ/mol [9], we adopt the basic function form of EAM proposed by Cai and Johnson [13, 14]. As to the Cu-W cross potential, we take the same function form proposed by the present authors while constructing the cross Cu-Ta potential [15]:

$$\phi_{CuW}(r) = A[\phi_{Cu}(r + B) + \phi_W(r + C)], \quad (1)$$

where r is the distance between Cu and W atoms. A, B, and C are three potential parameters to be fitted. It should be pointed out that to fit the Co-Ag and Cu-W cross potentials is a challenging issue, as there is no any equilibrium alloy phase in the systems and therefore no indispensable data available for fitting the cross potentials. In this respect, the first-principles calculation based on Quantum Mechanics is a reliable way for acquiring some physical properties of the equilibrium/nonequilibrium alloy phases with good precision. We, therefore, perform the first-principles calculations, based on the well-established Vienna *ab initio* simulation package (VASP) [16], to obtain the cohesive energies and lattice constants of some nonequilibrium alloy phases of the systems. The calculated data are then used in fitting the Co-Ag and Cu-W cross-potentials. After the fitting procedure and optimization of the potential parameters, Table II lists the fitted parameters for the Co-Co, Ag-Ag, and Co-Ag potentials, and Table III lists the fitted parameters for Cu-Cu, W-W, and Cu-W potentials. It should be pointed out that the constructed Co-Ag and Cu-W potentials work fairly well as they are capable of reproducing some physical properties of the Co-Ag and Cu-W systems, respectively (not shown here).

TABLE II Parameters for the Co-Co, Ag-Ag, and Co-Ag potentials

	A (eV)	ξ (eV)	P	Q	d (Å)
Co-Co	0.0950	1.4880	11.604	2.286	2.51
Ag-Ag	0.1028	1.178	10.928	3.139	2.89
Co-Ag	0.1040	1.3671	11.2118	2.7089	2.84

TABLE III Fitted parameters for the Cu-Cu, W-W, and Cu-W potentials

Cu-Cu		W-W		Cu-W	
χ	11.134231	χ	6.180480	A	0.362635
α (eV)	0.725977	k_0 (eV)	−0.581958		
β	3.457434	k_1 (eV)	−2.175060	B (Å)	−0.229870
r_a (Å)	1.629356	k_2 (eV)	17.053662		
F_1 (eV)	0.676073	k_3 (eV)	−8.215108	C (Å)	0.094444

3. Simulation models and characterization methods

In the present study, solid solution models are constructed for three major crystalline structures of fcc, bcc and hcp, i.e., the models consist of $8 \times 8 \times 8 \times 4 = 2048$ atoms for an fcc phase, $9 \times 9 \times 8 \times 2 = 1296$ atoms for a bcc phase, and $10 \times 6 \times 6 \times 4 = 1440$ atoms for a hcp phase, respectively. In fcc and bcc models, the [100], [010], and [001] atomic crystal directions are parallel to x, y, and z axis, respectively, and in the hcp model, the [100], [001] and [120] crystalline directions are parallel to x, y, and z axes, respectively. In all three directions, periodic boundary conditions are adopted.

Based on the constructed potentials, MD simulations are carried out with Parrinello-Rahman constant pressure scheme and the equations of motion are solved through a fourth-order predictor-corrector algorithm of Gear with a time step $t = 5 \times 10^{-15}$ s [17]. To simulate the fcc/bcc/hcp solid solution, the initial solid solution model is obtained by randomly substituting a desired amount of solvent atoms by solute atoms in the original lattice. The solid solution model is then run at a constant temperature 300 K to reach a relatively stable state, at which all the dynamic parameters show no secular variation. The amount of solute atoms is gradually increased to find out the critical compositions, at and beyond which the solid solutions would become energetically unstable and collapse into the corresponding disordered states.

The process of solid-state crystal-to-amorphous transition in the simulation model is monitored by the projections of the atomic positions, the planar structure factor S (**k, z**), the pair-correlation function $g(r)$, as well as the density profiles of each species along the z direction $\rho_\alpha(z)$.

4. Results and discussion

We first present the simulation results obtained from the equilibrium miscible Ni-Ta, Ni-Mo, and Ni-Ti systems [10–12]. Table IV lists the calculated critical solid solubilities and the glass forming ranges (GFR) of the Ni-Ta, Ni-Mo, and Ni-Ti systems. From the Table, it can be seen that the calculated GFRs of the Ni-Ta, Ni-Mo, and Ni-Ti systems are 43–79 at.% Ni [10], 25–79 at.% Ni [18], and 15–62 at.% Ni [12], respectively. Apparently, the calculated GFRs of Ni-Mo and Ni-Ti systems are in good agreement with the experimental GFR of 25–79 at.% Ni for the Ni-Mo system [19] and 15–62 at.% Ni for the Ni-Ti system [12], respectively.

For the equilibrium immiscible Co-Ag system, the critical compositions of the crystal-to-amorphous transition for both terminal solid solutions are revealed by MD simulations and the metallic glass-forming range of the Co-Ag system is therefore predicted to be within 12–82 at.% of Ag. As a typical example to show the determination of the critical composition, Fig. 1 exhibits the projections of atomic positions of $Co_{17}Ag_{83}$ and $Co_{18}Ag_{82}$ solid solutions after annealing at 300 K for 0.25 ns, respectively. It can be seen vividly that a uniform disordered structure is formed in the $Co_{18}Ag_{82}$ solid solution model, while the $Co_{17}Ag_{83}$

TABLE IV Critical solid solubilities and glass forming ranges (GFR) of some miscible binary metal systems determined by their respective potentials through MD simulations (units of the alloy composition are at.%)

	System		
	Ni-Ta	Ni-Mo	Ni-Ti
Potential	EAM	FS	TB
Solubility of Ni	21	21	38
Solubility of partner metal	43	25	15
Calculated GFR (Ni at.%)	43–79	25–79	15–62
Experimental GFR (Ni at.%)	Not available	25–75	15–62
Reference	[10]	[11, 18, 19]	[12]

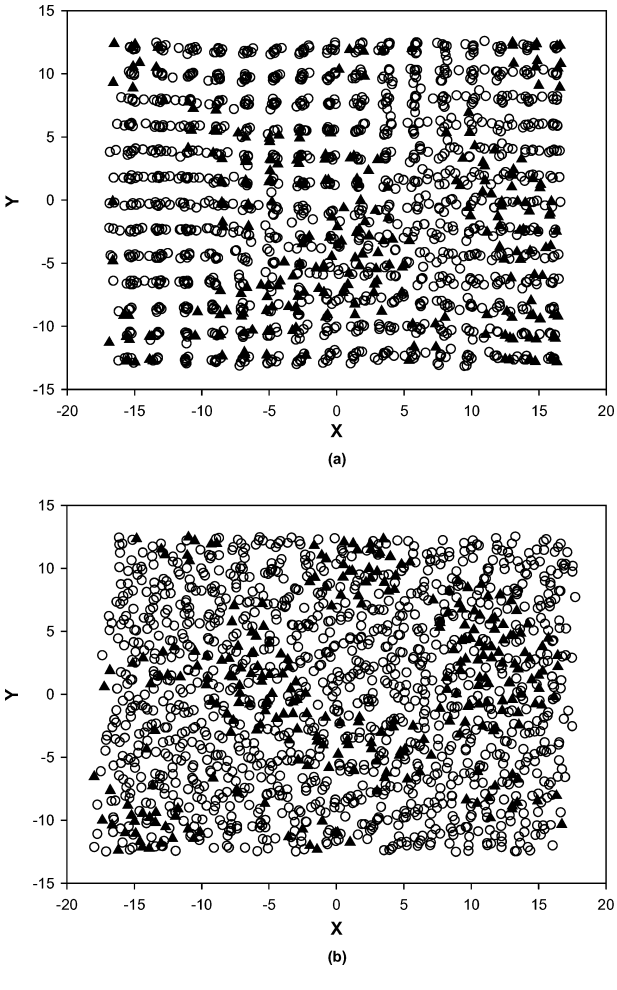

Figure 1 The projections of atomic positions of the Ag-based solid solutions after annealing at 300 K for 0.25 ns with different Co concentrations: (a) 17 at.%, showing some deformation in the crystalline solid solution, and (b) 18 at.%, showing an amorphous state. Solid triangles: Co. Open circles: Ag.

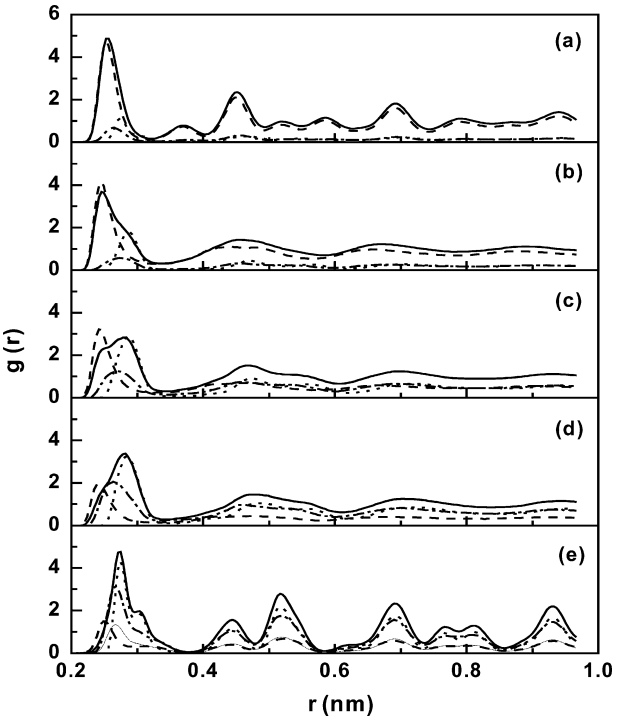

Figure 2 Partial and total pair correlation functions of (a) $Cu_{85}W_{15}$, (b) $Cu_{80}W_{20}$, (c) $Cu_{50}W_{50}$, (d) $Cu_{35}W_{65}$, and (e) $Cu_{30}W_{70}$ solid solutions after annealing at 300 K for 0.5 ns, respectively. The solid line is for the total $g(r)$, the dashed line is for Cu-Cu partial $g(r)$, the dotted line is for W-W partial $g(r)$, and the dash-dotted line is for Cu-W partial $g(r)$.

solid solution still remains in an ordered state, indicating that 18 at.% Co is a critical composition of the crystal-to-amorphous transition. It is certainly desirable to perform experimental studies to testify the above prediction, which is currently undertaken by authors' group with a far-from-equilibrium process of ion beam mixing.

For the equilibrium immiscible Cu-W system, similar MD simulations are conducted with solid solution models based on the newly constructed Cu-W potential and the intrinsic GFR is determined to be within 20 to 65 at.% of W. Fig. 2 displays the partial and total pair-correlation functions of the Cu-W solid solutions versus the alloy composition upon annealing at 300 K. From Fig. 2, one sees apparently that the $Cu_{85}W_{15}$ and $Cu_{30}W_{70}$ solid solutions still remain in crystalline structures, while the $Cu_{80}W_{20}$, $Cu_{50}W_{50}$, and $Cu_{35}W_{65}$ solid solutions all become amorphous, indicating that 20 and 65 at.% W, are two critical compositions of the crystal-to-amorphous transition in the Cu-W system. It is of interest to recall some experimental observations, which are in support of the above simulation results. For instance, Rizzo *et al.* have observed that the vapor-deposited Cu-W alloys containing 25 to 55 at.% W became completely amorphous [20]. It is noted that the GFR observed from experiments is very close to, and reasonably a little smaller than the intrinsic one of 20 to 65 at.% W derived by the present MD simulations.

5. Conclusion

We have shown that the glass-forming ability/range of a binary metal system is directly determined by its inter-atomic potential, which governs the energetic states of the solid solution and its competing disordered counterpart, thus determining which state is favored as a function of the alloy composition. We have also shown that for an equilibrium immiscible system characterized by a large positive heat of formation, *ab initio* calculation could be of help in providing some necessary physical date in deriving its inter-atomic potential, as there is no any equilibrium alloy existing in the system. It is demonstrated that the calculated GFAs/GFRs are in good agreement with the experimental observations in some representative systems.

Acknowledgements

The authors are grateful to the financial support from the National Natural Science Foundation of China, The Ministry of Science and Technology of China (G20000672), as well as from Tsinghua University.

References

1. W. KLEMENT, R. H. WILLENS and P. DUWEZ, *Nature* **187** (1960) 869.
2. B. X. LIU, W. L. JOHNSON, M.-A. NICOLET and S. S. LAU, *Appl. Phys. Lett.* **42** (1983) 45.
3. R. B. SCHWARZ and W. L. JOHNSON, *Phys. Rev. Lett.* **51** (1983) 415.
4. B. X. LIU, W. S. LAI and Q. ZHANG, *Mater. Sci. & Eng.* R **244** (2000) 1.
5. B. X. LIU, W. S. LAI and Z. J. ZHANG, *Adv. in Phys.* **50** (2001) 367.
6. M. S. DAW and M. I. BASKES, *Phys. Rev. Lett.* **50** (1983) 1285.
7. M. W. FINNIS and J. E. SINCLAIR, *Philos. Mag.* A **50** (1984) 45.
8. D. TOMANEK, A. A. ALIGIA and C. A. BALSEIRO, *Phys. Rev.* B **32** (1985) 5051.
9. F. R. DE BOER, R. BOOM, W. C. M. MATTENS, A. R. MIEDEMA and A. K. NIESSEN, "Cohesion in Metals: Transition Metal Alloys" (North-Holland, Amsterdam, 1989).
10. Q. ZHANG, W. S. LAI and B. X. LIU, *Phys. Rev.* B **61** (2000) 9345.
11. *Idem.*, *ibid.* **58** (1998) 14020.
12. W. S. LAI, Q. ZHANG, B. X. LIU and E. MA, *J. Phys. Soc. Jpn.* **69** (2000) 2923.
13. J. CAI and Y. Y. YE, *Phys. Rev.* B **54** (1997) 8398.
14. R. A. JOHNSON and D. J. OH, *J. Mater. Res.* **4** (1989) 1195.
15. H. R. GONG, L. T. KONG, W. S. LAI and B. X. LIU, *Phys. Rev.* B **66** (2002) 104204.
16. G. KRESSE and J. HAFNER, *ibid.* **47** (1993) 558.
17. M. PARRINELLO and A. RAHMAN, *J. Appl. Phys.* **52** (1981) 7182.
18. Q. ZHANG, W. S. LAI and B. X. LIU, *Phys. Rev.* B **59** (1999) 13521.
19. Z. J. ZHANG and B. X. LIU, *J. Appl. Phys.* **76** (1994) 3351.
20. H. F. RIZZO, T. B. MASSALSKI and M. NASTASI, *Metall. Trans.* A **24A** (1993) 1027.

Received 11 September 2003
and accepted 27 February 2004